Winter 12-6-2016

INFLAMMATORY GENE EXPRESSION IN WOMEN DIAGNOSED WITH POLYCYSTIC OVARIAN SYNDROME

Myles K. Taylor
Pittsburg State University, mtaylor@gus.pittstate.edu

INFLAMMATORY GENE EXPRESSION IN WOMEN DIAGNOSED WITH POLYCYSTIC OVARIAN SYNDROME

A Thesis Submitted to the Graduate School
in Partial Fulfillment of the Requirements
for the Degree of
Master of Science

Myles K. Taylor

Pittsburg State University

Pittsburg, Kansas

December, 2016

INFLAMMATORY GENE EXPRESSION IN WOMEN DIAGNOSED WITH POLYCYCSTIC OVARIAN SYNDROME

Myles K. Taylor

APPROVED:

Thesis Advisor _____
Dr. Peter Chung, Department of Biology

Committee Member _____
Dr. Neal Schmidt, Department of Biology

Committee Member _____
Dr. Barbara McClaskey, Department of Nursing

INFLAMMATORY GENE EXPRESSION IN WOMEN DIAGNOSED WITH POLYCYSTIC OVARIAN SYNDROME

An Abstract of the Thesis by
Myles K Taylor

Polycystic ovarian syndrome (PCOS) is a common endocrine disorder in women of reproductive age. The pathophysiology of PCOS has conventionally thought to originate from androgen excess. However, recent evidence suggests that androgen excess is a downstream consequence to inflammatory dysregulation and subsequent metabolic abnormalities. Inflammatory mRNA gene expression of TNFα and IL-1ß in mononuclear cells isolated from women diagnosed with PCOS was explored using qPCR. Also, the correlations between body mass index (BMI) and fasting glucose on mRNA expression of TNFα and IL-1ß were explored. mRNA expression of both TNFα and IL-1ß were found to be significantly higher in PCOS subjects ($P<0.01$). BMI was found to significantly increase mRNA expression of TNFα and IL-1ß ($P<0.05$). However, only mRNA expression of TNFα was found to correlate with fasting glucose ($P<0.05$).

TABLE OF CONTENTS

CHAPTER		PAGE
I.	INTRODUCTION	1
	PCOS	1
	Body Composition and Inflammation	3
	Inflammation and Insulin Resistance	5
	Inflammation and Hyperandrogenism	7
	Body Composition-Independent Inflammation	7
	Current Therapies	9
	Purpose of Research	9
II.	MATERIALS AND METHODS	10
	Subjects	10
	Body Composition	10
	Biochemical Analysis	10
	Mononuclear Cell Isolation	11
	RNA Isolation	11
	cDNA Synthesis	13
	Primer Design and Kinetics Validation	13
	Quantitative PCR	15
	Reference Gene Stability and Relative Gene Expression	16
	Statistics	17
III.	RESULTS	18
	Age, BMI, and Fasting Glucose	18
	Isolated Total RNA Purity and Integrity	18
	Primer Kinetic Efficiency	19
	geNorm and qBase+	22
	MNC-Derived TNFα and IL-1ß Expression	23
IV.	DISCUSSION	28
REFERENCES		31
APPENDIX		34

LIST OF TABLES

TABLE		PAGE
Table 1.	Rotterdam Criteria 2003	2
Table 2.	Forward and Reverse Primer Sequence and Product Size	14
Table 3.	Age, Body Composition, and Fasting Glucose of Subjects	18
Table 4.	Assay PCR Kinetic Efficiency	21
Table 5.	Relative Quantity of TNFα and IL-1ß	23

LIST OF FIGURES

FIGURE		PAGE
Figure 1.	1.2% Agarose RNA Gel Electrophoresis	19
Figure 2.	Correlation of Cq and DNA Input Amount	20
Figure 3.	Dissociation Curve	21
Figure 4.	3% Agarose Gel Electrophoresis	22
Figure 5.	Mononuclear Cell Cytokine Expression	23
Figure 6.	Mononuclear Cell Cytokine Expression	24
Figure 7.	Correlation Between BMI and Cytokine Expression	24
Figure 8.	Correlation Between BMI of Women with PCOS and Cytokine Expression	25
Figure 9.	Correlation Between Fasting Glucose and Cytokine Expression	26
Figure 10.	Correlation Between Fasting Glucose of Women with PCOS and Cytokine Expression	26

CHAPTER I

INTRODUCTION

Polycystic Ovarian Syndrome

Polycystic ovarian syndrome (PCOS), first identified in 1935 by Dr. Stein and Leventhal, is a common endocrine disorder affecting women of childbearing years [1]. Approximately 4 to 7 percent of women are affected. Women affected by PCOS are more likely to receive care for heart disease, diabetes, and mental health conditions. $4.36 billion dollars are spent annually on the care for women with PCOS [2]. Currently, the etiology of PCOS is poorly understood. However, recent literature has suggested inflammatory dysregulation in mononuclear cells (MNC) plays a significant role in the early stages of PCOS.

Clinical manifestations associated with PCOS are very broad and are not limited gynecological issues. Diagnosis of PCOS is highly disputed among medical professions due to several similarities with other pathologies. No single definitive diagnostic test exists for PCOS, rather, a collective of physical and biochemical signs is considered for diagnosis. Rotterdam criteria (**Table 1**) are the most commonly used guidelines for diagnosis of PCOS [3-5]. Obesity and insulin resistance, although not considered diagnostic criterion of PCOS, are highly prevalent among women with PCOS, and

contribute long-term health risks such as cardiovascular disease, type 2 diabetes, and dyslipidemia [3, 4, 6].

Rotterdam Criteria 2003
1. Oligo-and/or anovulation 2. Clinical and/or biochemical signs of hyperandrogenism 3. Polycystic ovaries (Two of three criteria needed)

Table 1. Rotterdam Criteria 2003

The majority of physical manifestations experienced in PCOS are the result of excess androgen hormones. Hair follicles and sebaceous glands are androgen-dependent structures and are commonly affected by the increased androgens in PCOS leading to hirsutism, pattern baldness, and acne [5, 7].

PCOS represents a complex pathophysiological model with no single causative agent currently determined. Rather, multiple factors contributing to the signature biochemical feature of hyperandrogenism. Excess androgens are the main culprit behind the majority of clinical features of PCOS [5].

Several abnormalities in ovarian physiology occur in women with PCOS. Anti-Müllerian hormone (AMH) is secreted by granulosa cells (GC) and plays a significant role in folliculogenesis. AMH is commonly elevated in PCOS and arrests the progression towards ovulation through inhibition of primodial follicle initiation and sensitivity to follicle-stimulating hormone (FSH) [8]. Poor fertility outcomes are in women with PCOS due to ovulation inhibition. Chronic absence of ovulation encourages the continual endometrial stimulation by estrogen, increasing the risk of endometrial hyperplasia and endometrial cancer [6, 9].

Abnormalities in hypothalamus-hypophysis-ovary axis feedback resulting in greater secretion of luteinizing hormone (LH) is another common feature of PCOS. Elevated LH stimulates ovarian theca cells (TC) to over synthesize androgens resulting in hyperandrogenism. Hypoandrogenism decreases the feedback inhibition of progesterone and estradiol leading to greater secretion of LH. Disturbances in feedback mechanisms perpetuates a pathophysiological cycle of hyperandrogenism [5, 10].

Although hyperandrogenism is the culprit for the majority of the clinical manifestations in PCOS, the primary pathophysiological changes in PCOS are poorly understood. Insulin resistance may play an important upstream role in androgen dysregulation. In normal populations, insulin resistance is most commonly associated with obesity related inflammation. While the majority of women with PCOS are classified as obese, a small portion have normal body compositions in addition to insulin resistance. Therefore, obesity is most likely not the primary cause of insulin resistance. Recent literature has suggested that inflammatory dysregulation in MNCs independent of body composition contributes to insulin resistance in PCOS [11, 12].

Body Composition and Inflammation

Obesity poses a significant public health risk with nearly 80 million people affected in the United States. Approximately 69% of adults are overweight with 35% classified as obese. Significant increases in developing chronic diseases such as type 2 diabetes mellitus, hypertension, and chronic heart disease are associated with obesity. Clinical guidelines identify obese individuals as a body mass index $\geq$30 kg/m^2 [13, 14]. The majority of women diagnosed with PCOS have elevated BMI with approximately

70% classified as obese. However, there remains a small portion of women with PCOS who fall within a normal BMI range [15, 16]. Obesity is well defined as a significant inflammatory stimulus and contributor to the development of insulin-resistance and type 2 diabetes. However, the role of obesity in the pathogenesis of PCOS remains unknown. Despite this, it is likely that when obesity is present with PCOS, reproduction, and metabolic aberrations are more prevalent [17].

Unlike the common features of swelling, redness and pain found in an acute inflammatory response due to tissue injury, obesity-related inflammation is derived from metabolic stimuli and maintained at subacute levels. Substantial differences in adipocytokine expression exist between adipose tissue from lean and obese individuals. Adipose tissue from obese individuals expressed greater amounts of inflammatory TNFα and IL-1ß. TNFα and IL-1ß are major contributors to the development of glucose intolerance and insulin resistance, as well as atherosclerosis [18-20]. Conversely, tissue from normal weight individuals expressed greater amounts of cytokines of anti-inflammatory nature, such as IL-4 [21, 22]. Adipocytokines heavily mediate immune and inflammatory responses through epigenetic modifications of hematopoietic cells [23, 24].

Macrophage, derived from monocytes, are the potent mediators of inflammation through the secretion of cytokines. Two major phenotypes of macrophages exist, inflammatory M1 phenotype and anti-inflammatory M2 phenotype. Though, this view is simplistic. Depending on the signaling environment, individual macrophage exhibit various degrees of inflammatory and anti-inflammatory nature, and must be sustained in a similar environment to exhibit that phenotype. In obese individuals, increased expression of inflammatory cytokines in adipose tissue promotes the M1 phenotype.

Consequently, a shift towards the M1 phenotype increases the inflammatory environment through the increased production of inflammatory cytokines. Whereas, adipose tissue from lean individuals expresses an anti-inflammatory environment, shifting towards the M2 phenotype. By producing cytokines of anti-inflammatory nature, M2 macrophage maintain an anti-inflammatory environment [25-29]. Interestingly, M1 and M2 macrophage phenotypes have different preferred energy substrates. Glucose is the primary substrate used by M1 macrophages. M2 macrophage prefers fatty acids as an energy substrate. Also, macrophages primarily use insulin-independent glucose transporters despite having a functional insulin receptor. Insulin-independent glucose uptake becomes interesting when insulin resistance and hyperglycemia are present, and uptake and utilization of glucose remain normal in macrophage [25, 30-32].

Inflammation and Insulin Resistance

Inflammation is well understood to be a major contributor to the development of insulin resistance in insulin-sensitive tissues. Cytokines are capable of acting in an endocrine fashion if secreted into the blood stream. As obesity increases and subsequent cytokine production increases, inflammatory mediators can enter the blood stream and travel to peripheral tissues leading to insulin resistance within insulin sensitive tissues. Of particular interest, the cardinal inflammatory cytokine TNFα has been shown to directly inhibit proper insulin signaling through interactions with insulin receptor substrate-1 (IRS-1). Binding of TNFα to the TNFα receptor leads the activation of JNK and IKK and subsequent phosphorylation of IRS-1 serine residues. Consequently, the IRS-1 function is decreased, decreasing the activation of phosphoinositide 3-kinase (PI3K) [33-35].

Decreased activity of PI3K results in the inhibition of protein kinase B (Akt2), which is responsible for the translocation of the insulin-dependent glucose transporter GLUT-4. Under normal insulin signaling, Akt leads to the suppression of gluconeogenesis through inhibition of FoxO1. When abnormal signaling occurs, and Akt activation decreases, FoxO1 functions normally and gluconeogenesis continues. Consequently, plasma glucose begins to rise as gluconeogenesis continues and remains at hyperglycemic concentrations due to the decreased uptake of glucose into the cell by GLUT-4 [36].

Maintaining a hyperglycemic state has several consequences to various tissues. Most notably are the destruction of pancreatic ß-cells which are responsible for the production of insulin. As a compensatory mechanism, hyperglycemia stimuli signal ß-cells to increase the production and secretion of insulin. If this is allowed to continue, ß-cells will eventually die, leading to type 2 diabetes mellitus and the necessity of supplying exogenous insulin.

Hyperglycemia also contributes to promoting an inflammatory state through the preferred bioenergetic pathway of M1-like macrophages. Despite the presence of insulin-resistance, uptake of glucose by M1-like macrophages is maintained through insulin-independent transporters and used as an energy substrate in mitochondrial respiration. Reactive oxygen species is a strong signal for transcription of inflammatory mediators and is primarily produce from NAPDH oxidase during mitochondrial respiration. Consequently, another source of inflammation is added and contributes to the cyclical nature of inflammation and insulin resistance [37].

Insulin and Hyperandrogenism

Insulin, in addition to glucose homeostasis, regulates GnRH and LH secretion from the pituitary and transcription of the androgen synthesizing enzymes in the ovaries. While insulin resistance and hyperinsulinemia develops in peripheral tissues, the pituitary and ovaries remain highly sensitive to insulin in PCOS. Increased LH secretion consequently augments steroid synthesis in the ovaries. In the ovaries, physiological doses of insulin are capable of inducing synthesis of androgens though increase acute steroidogenic regulatory protein (StAR) in women with PCOS. Much larger doses of insulin are required to elicit the same response in normal women [38-40]. Insulin also increases the activity of 17-α-hydroxylase/17,20-lyase, 3-ß-hydroxysteroid dehydrogenase, and aromatase leading to excess production of progesterone, 17-α-hydroxyprogesterone, and testosterone [5, 41].

Body Composition-Independent Inflammation in PCOS

Obesity is a significant promoter of inflammation and insulin-resistance. However, recent studies show that women with PCOS demonstrate elevated inflammatory markers and insulin resistance independent of obesity. Compared to BMI-matched controls, women with PCOS have higher circulating levels of TNF and IL-1ß. However, when obesity is present with PCOS, these cytokines are elevated to a greater degree [11, 12, 42]. Distribution and physiology of adipose tissue may provide an explanation for increased inflammatory markers and insulin resistance in normal weight women with PCOS. A large DXA population study found that women with PCOS preferentially store visceral adipose in the abdominal region, leading to increased android

adiposity in normal weight women. Increased android fat mass in normal weight women with PCOS positively correlated with serum insulin and androgens [15, 43]. However, increased android adiposity cannot explain insulin resistance and increased inflammation in all PCOS cases, particularly lean women.

Insulin resistance and increased inflammation in the absence of excess adiposity is found in lean women with PCOS, suggesting inflammation is not originally derived from adipose tissue. Rather, evidence suggests that the inflammatory response is nutrient-induced. Mononuclear cells (MNC) were isolated from lean and obese women with PCOS and their matching controls during a glucose tolerance test. IL-6, TNFα, and IL-1ß were assayed from MNC after culturing for 24hr. MNC from both lean and obese women with PCOS were found to secrete greater amounts of IL-6, TNFα and IL-1ß compared to their counterparts. The similar inflammatory response was observed when challenged with lipids rather than glucose [11, 12, 44].

Utilizing glucose tolerance testing provides a practical in vivo model simulating daily nutrient intake. However, the inflammatory cytokines were assayed from cell culture supernatant after culturing for 24hr. Assaying cytokines in this ex vivo fashion does not completely represent the inflammatory response of the individual. Also, only secreted cytokines were assayed, and does not take into account intracellular cytokines. Although, the observed increase in cytokine production among PCOS groups compared to normal controls indicates inflammatory dysregulation.

Current Therapies

Due to poor understanding of underlying pathogenesis, therapeutic options are limited for PCOS. Treatment is often limited to lifestyle modifications, insulin sensitizing agents, and oral contraceptives. Diet and exercise for weight loss are the first choice for overweight and obese individuals. However, diet and exercise as a monotherapy has very limited efficacy. Metformin, commonly used for type 2 diabetes, is used to treat insulin resistance in PCOS. Yet, long-term efficacy is poor [45]. Contraceptives containing estrogen and progestin derivatives are commonly prescribed to treat symptoms of excess androgens. However, use of hormonal contraceptives come with several unwanted side effects, including limiting the ability to conceive [6].

Purpose of this Research

Polycystic ovarian syndrome represents a complex pathophysiological model of cyclical nature. Poor understanding of PCOS pathophysiology has greatly limited therapies available to clinicians. Previous work exploring inflammatory cytokine expression in PCOS have been limited to post translation analysis The objective of this study is to evaluate transcriptional mRNA expression of inflammatory cytokines TNFα and IL-1ß and their correlation to metabolic disturbances in women with PCOS.

CHAPTER II

MATERIALS AND METHODS

Subjects

Thirty-nine women, 25 with PCOS (5 non-obese, 20 obese) and 14 without PCOS (9 non-obese, 5 obese), 18-55 years of age volunteered for this study. Non-obese and obese were defined as having a BMI of <30 and >30 kg/m^2, respectively. Subjects were enrolled through the medical practice of Patricia Sullivan, NP-C. All study subjects were screened using Rotterdam criteria. PCOS subjects were selected by meeting two of the criteria in **Table 1**. Control subjects had normal ovulation and did not exhibit physical manifestations of excess androgens. Subjects taking medications for metabolic conditions were excluded from the study. The Pittsburg State University Institutional Review Board provided approval for the study. Informed consent was obtained from all participants prior to sample collection.

Body Composition

Height and body weight were recorded with a height rod and beam scale. Height was measured to the nearest 1.0 in and body weight was measured to the nearest 1.0 lb. Body mass index was calculated from measured height and weight.

Biochemical Analysis

After a 12 hour overnight fast, 24 mL of blood was obtained from an antecubital vein to measure serum glucose and to isolate MNCs. Twenty mL of blood was treated with K2 EDTA to prevent coagulation for isolation of MNCs. The remaining 4 mL of blood was allowed to clot and centrifuged at 1,000 x g for 10 minutes to remove the clot. Fasting serum glucose was determined by hexokinase G-6-PDH methodology (Mag Lab Medical Laboratory, Pittsburg, KS). MNC relative gene expression of TNFα and Il1ß was determined by quantitative polymerase chain reaction (qPCR) and SYBR green chemistry.

Mononuclear Cell Isolation

Immediately after collection, uncoagulated blood samples were diluted with an equal volume of phosphate buffered saline (PBS), inverted several times to mix thoroughly. Diluted blood was then carefully layered upon Lymphoprep density gradient media and centrifuged at 10˚C for 30 minutes at 800 x g with the brake off. The buffy coat containing mononuclear cells was collected and washed with PBS. Mononuclear cells were pelleted at 10˚C for 10 minutes at 1200 x g. The PBS supernatant was removed and the remaining cell pellet was lysed in 1 mL of TRI-Reagent BD (MRC) and transferred to a 1.7 mL microfuge tube.

RNA Isolation

Before isolating RNA, benchtop and pippettors were thoroughly cleaned and treated with RNase Away (Ambion). Phase separation was performed by adding 200 µL

of chloroform, mixed vigorously by hand for 15 seconds and centrifuged at 4˚C for 15 minutes at 12,000 x g. 400 µL of the RNA containing aqueous layer was removed and transferred to a new 1.7 microfuge tube. An equal volume of 99% ethanol was added to the aqueous layer and transferred to a Direct-Zol (Zymo Research) RNA isolation column. All centrifugation steps were performed at 12,000 x g. The column was centrifuged for 30 seconds, discarding the flow through. 400 µL of RNA wash was added to the column and centrifuged for 30 seconds, discarding the flow though. The column was transferred to a new collection tube. An on column DNA digest was performed to remove residual gDNA with DNase I for 15 minutes. 400 µL of preRNA wash was added to the column and centrifuged for 30 seconds, discarding the flow. This step was performed for a second time. 700 µL of RNA wash was added and centrifuged for 1 min. The Direct-zol column was then transferred to a microfuge tube. 50 µL of nuclease free water was added to the column matrix and incubated for 1 minute and centrifuged for 1 minute. RNA concentration and purity was quantified with a NanoDrop lite analyzer. Isolated total RNA was stored at -80˚C.

RNA integrity was determined by gel electrophoresis right before cDNA synthesis. Five µL of isolated total RNA was heated to 95˚C for 1 min and immediately put on ice. A 1.2% agarose gel was made by heating 0.6 g of agarose in 50 mL of 1x TAE buffer. 2 µL of ethidium bromide was added to the mixture. The solution was then poured into a casting tray to solidify. After solidifying, the agarose gel was transferred to an electrophoresis chamber and the chamber was filled with 1x TAE buffer until covering the top of the agarose gel. Five µL of 6x loading dye was added to each RNA sample and

loaded into the agarose gel. Electrophoresis was performed at 90V for 30 minutes. The gel was then imaged on a FluroChem E under UV light.

cDNA Synthesis

cDNA was synthesized from 2 µg of isolated total RNA using SuperScript IV VILO master mix (Invitogen). SuperScript IV VILO contains a mixture of oligo-dT and random hexamers. 4 µL of SuperScript IV VILO master mix, variable volume of template RNA for 2 µg of total RNA, and variable volume of nuclease free H_2O to bring the final volume to 20 µL. Reaction was thoroughly mixed by pipetting. Thermal cycling condition were 25˚C for 10 minutes, 50˚C for 10 minutes, and 85˚C for 5 minutes. Synthesized cDNA was diluted with nuclease free water to obtain a concentration of 10 ng/µL and separated in several aliquots to prevent multiple freeze thaw cycles. Diluted cDNA samples were stored at -20˚C.

Primer Design and Kinetics Validation

Primers for TNFα, IL-1ß, TBP, and SDHA were selected based on product size, exon spanning, and primer annealing temperatures above 60˚C. Selected primer sequences were analyzed by Primer-Blast (NCBI) for specificity and amplicon size. Sequences and product sizes are shown in **Table 2**. Primers were synthesized by Integrated DNA Technologies and supplied in 100 nmol stock concentration. Several aliquots of 10 pmol primer solution were prepared by 1:10 dilution of the 100 nmol stock solution to prevent freeze/thaw degradation of primers. Primers were stored at -20˚.

Target			Product Size
TNF	Forward	5’-CCTGCCCCAATCCCTTTATT-3’	81 bp
	Reverse	5’-CCCTAAGCCCCCAATTCTCT-3’	
IL-1ß	Forward	5’-ATGATGGCTTATTACAGTGGCAA-3’	132 bp
	Reverse	5’-GTCGGAGATTCGTAGCTGGA-3’	
TBP	Forward	5’-TGCACAGGAGCCAAGAGTGAA-3’	132 bp
	Reverse	5’-CACATCACAGCTCCCCACCA-3’	
SDHA	Forward	5’-TGGGAACAAGAGGGCATCTG-3’	86 bp
	Reverse	5’-CCACCACTGCATCAAATTCATG-3’	

Table 2. Forward and Reverse Primer Sequence and Product Size

A gBlock® Gene Fragment (Integrative DNA Technologies) containing each PCR amplicon was synthesized and diluted to 100 pg/mL to serve as a positive control, reference sample, and inter-run calibrator. Several aliquots of the synthetic DNA template were made to prevent multiple freeze/thaw cycles and stored at -20˚C. Kinetic efficiencies for each PCR assay was determined from a sevenfold dilution series of the synthetic DNA template. The first concentration of the dilution series was 100 pg/mL. Several 1:10 dilutions were made until a final concentration of 0.0001 pg/mL. In a clean biosafety cabinet, PCR reactions were prepared by combining 10 µL of PowerUp SYBR Green master mix (Invitrogen), 0.4 µL of 10 pmol forward primer, 0.4 µL of 10 µL reverse primer, 7.2 µL of nuclease free H_2O, and 2 µL of template for a final reaction volume of 20 µL. A no template control was prepared by replacing template DNA with nuclease free H_2O. PCR reactions were prepared in triplicate, pipetted into a 48 well qPCR optical plate, and sealed with optical adhesive film. Reaction plates were centrifuged at 500 x g for 1 minute to collect reaction mixture and remove bubbles formed from pipetting. qPCR was performed using an Applied Biosystems StepOne qPCR machine. Thermal cycling conditions were 50˚C for 2 minutes to activate UDG,

95˚C for 2 minutes for initial DNA denaturation, followed by 40 cycles of 95˚C for 3 seconds and an annealing/extension temperature of 60˚C for 30 seconds. SYBR green fluoresces was measured after each annealing/extension step. A dissociation melting curve was included after the last annealing/extension step. Baseline and threshold Cq settings were determined by the Applied Biosystems native software. Reaction replicates were averaged and plotted against the $\log_{10}$ of template input. Kinetic efficiencies were calculated from the slope of the trend line using eq 1 [46].

$$\text{Efficiency} = 10^{(-1/\text{slope})} \quad \text{(eq. 1)}$$

After performing a dissociation melting curve, the PCR product was electrophoresed on a 3% agarose gel to ensure one product and absence of primer dimer formation. 1.5 g of agarose was heated in 50 mL of 1x TAE buffer until boiling. 2 µL of ethidium bromide was added and poured into a casting tray to cool. After solidifying, the agarose gel was transferred to an electrophoresis chamber and covered in 1x TAE buffer. 5 µL of 6x loading dye was added to each PCR reaction and loaded into the agarose gel. Electrophoresis was performed at 60V for 90 minutes. After electrophoresis, the agarose gel was imaged on an FluroChemE under UV light.

Quantitative PCR

After assay efficiency was determined, qPCR was performed on cDNA samples derived from subject MNCs to determine relative expression of TNFα and IL-1ß using TBP and SDHA as reference genes to normalize cDNA input. One target was run per

PCR run to maximize plate efficiency and conserve reagents. Using the synthetic template as a reference sample, positive control, and inter-run calibrator, inter-run variance can be accounted for and targets on separate runs can be compared.

In a clean biosafety cabinet, PCR reactions prepared by combining 10 µL of PowerUp SYBR green master mix, 0.4 µL of forward primer, 0.4 µL of reverse primer, 7.2 µL of H_2O, and 2 µL of sample template for a final volume of 20 µL. A no template control was included on each plate. Each reaction was prepared in triplicate, pipetted into the 48 well qPCR optical plate, and sealed with optical adhesive film. qPCR optical plates were centrifuged at 500 x g for 1 min to collect reaction and remove bubbles introduced from pipetting. qPCR was performed using an Applied Biosystems StepOne qPCR machine. Thermal cycling conditions were 50˚C for 2 minutes to activate UDG, 95˚C for 2 minutes for initial DNA denaturation, followed by 40 cycles of 95˚C for 3 seconds and an annealing/extension temperature of 60˚C for 30 seconds. SYBR green fluoresces was measured after each annealing/extension step. A dissociation melting curve was included after the last annealing/extension step. Baseline and threshold Cq settings were adjusted to Cq threshold determined from primer validation.

Reference Gene Stability and Relative Gene Expression

Cq data across fourteen experiments were uploaded into qBase+ 3.0 (Biogazelle) to determine reference gene stability and relative gene expression of TNFα and IL-1ß. Sample replicates with Cq variance of ≥ 0.5 were excluded from data analysis. TBP and SDHA were used to normalize variance in cDNA input. Assay PCR kinetic efficiencies were included in data calculation to account for variation in efficiencies.

Statistics

Data were analyzed by SPSS Statistics (IBM Analytics). Relative gene expression data was log transformed to meet normality requirements. One-Way ANOVA was used to compare relative gene expression between women with PCOS and control women followed by LSD post hoc to compare subgroups. Correlation analysis was performed by single and multiple linear regression. Significance was accepted as $P \leq 0.05$.

CHAPTER III

RESULTS

Age, BMI, and Fasting Glucose

Subjects age, height, weight, and BMI (**Appendix 1**) were obtained prior to collecting sample collection. Fasting glucose (**Appendix 1**) values and peripheral mononuclear cells were obtained after fasting 12 hours prior. BMI was significantly ($P \leq 0.001$) different between obese and non-obese subjects regardless of PCOS (**Table 3**). Fasting glucose was similar among all subjects. Age was significantly ($P \leq 0.001$) different among all subjects.

	PCOS		**Control**	
	Non-Obese (n=5)	Obese (n=20)	Non-Obese (n=9)	Obese (n=5)
Age (y)	40±14	31±7	19±2	24±8
BMI (kg/m)	26±3	43±6	25±2	39±8
Glucose (mg/dL)	90±3	95±16	89±6	90±2

Table 3. Age, Body Composition, and Fasting Glucose of Subjects. Values are expressed as means ± SD.

Isolated Total RNA Purity and Integrity

Total RNA from peripheral mononuclear cells was isolated using phenol-chloroform phase separation and silica spin column methodology. A NanoDrop Lite

spectrophotometer was used to quantify total RNA concentration and purity. Protein contamination was minimal with 260/280 nm ratios between 1.8 and 2.0 for all samples. Intact 16s and 28s rRNA bands were observed for all samples after separation by electrophoresis on a 1.2% agarose gel (**Figure 1**), indicating minimally degraded RNA prior to cDNA synthesis.

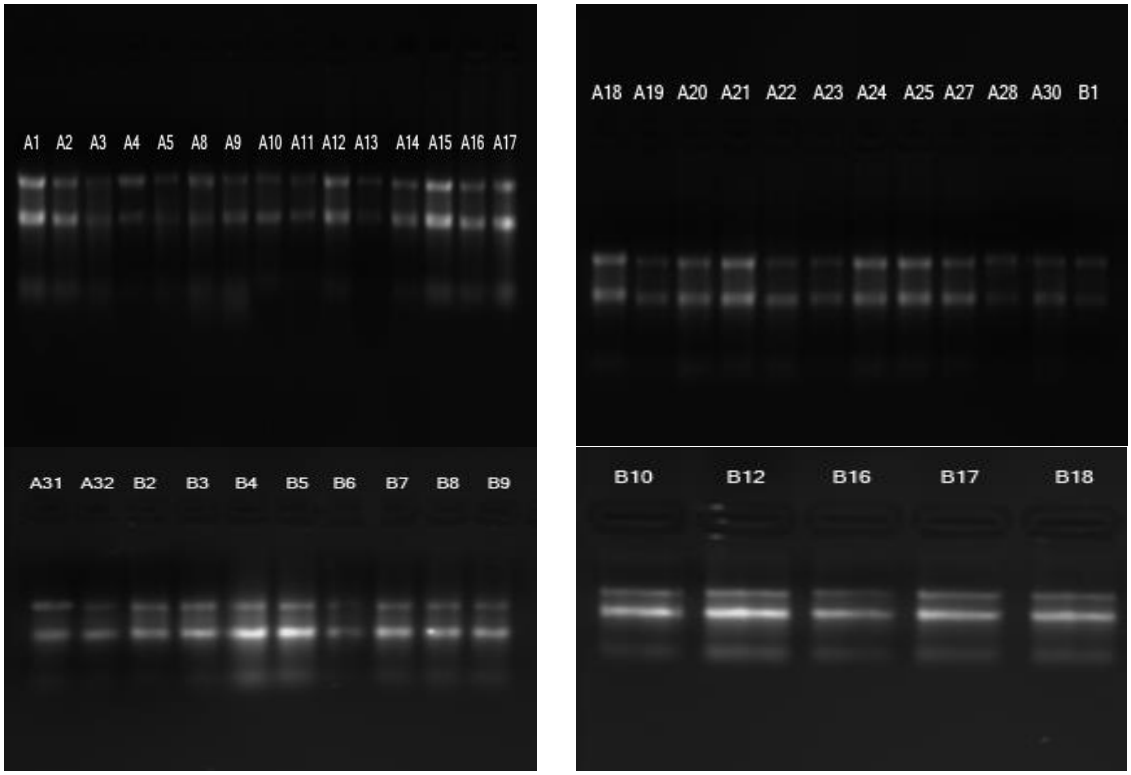

Figure 1. 1.2% RNA Gel Electrophoresis

Primer kinetic efficiencies

Replicate Cq values for each dilution were averaged and plotted against the $\log_{10}$ value of the input DNA amount (**Figure 2**). PCR kinetic efficiencies (**Table 4**) were calculated from the slope of the trend line using eq 1. All assays fell between 86-93% efficiency. Linearity ($R^2 \geq 0.999$) was observed for each assay across the dilution series

indicating PCR inhibitors were minimal. Dissociation curve analysis (**Figure 3**) revealed a single melting peak for each assay representing a single PCR product. Gel electrophoresis (**Figure 4**) further indicated a single PCR product and the absence of primer dimer formation.

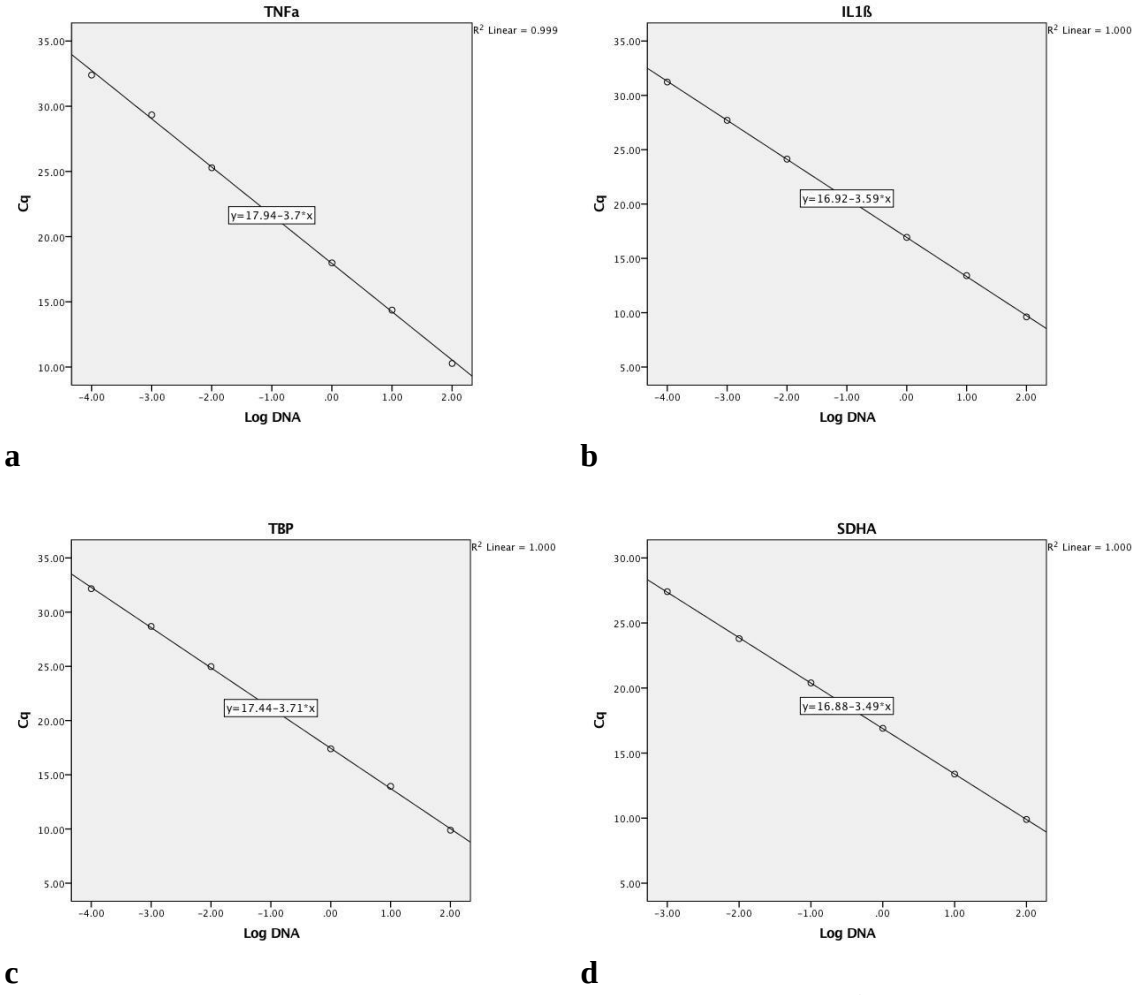

Figure 2. Correlation of Cq and DNA Input Amount a, TNFα $R^2 \geq 0.999$ **b**, IL-1ß $R^2=1.000$ **c**, $R^2=1.000$ **d**, $R^2=1.000$

	Efficiency
TNFα	1.86
IL-1ß	1.89
TBP	1.86
SDHA	1.93

Table 4. Assay PCR Kinetic Efficiency

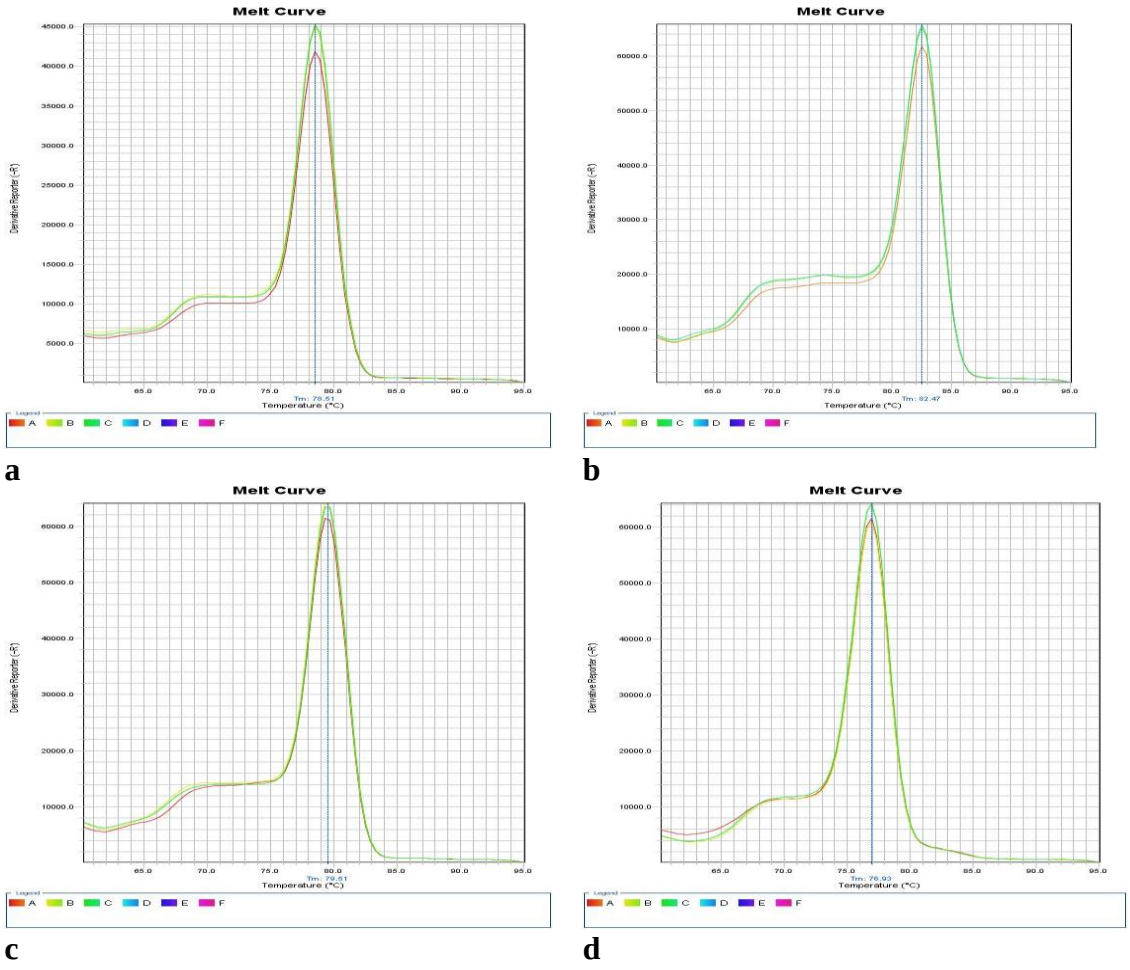

Figure 3. Dissociation Curve. a, TNFα **b**, IL-1ß c. TBP d. SDHA

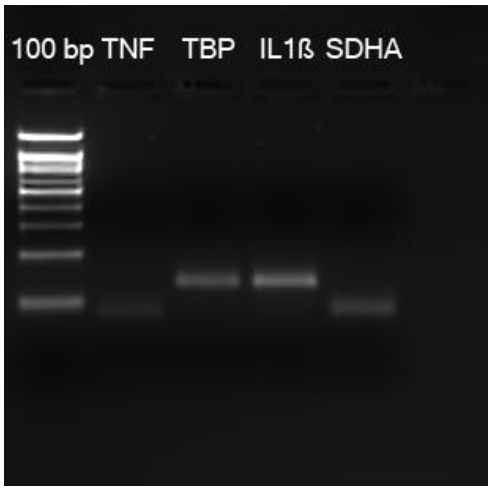

Figure 4. 3% Agarose Gel Electrophoresis of PCR Product

geNorm and qBase+

qPCR data across fourteen experiments was uploaded to qBase+. Two sample replicates out of 176 were removed for exceeding variance cutoff of >0.5 Cq. Relative gene expression of TNFα and IL-1ß was quantified by normalizing to reference genes TBP and SDHA (**Table 5**). geNorm analysis (CV=0.198) indicates stability of both reference genes across all samples.

Sample	TNFa RQ	IL-1ß RQ	Sample	TNFa RQ	IL-1ß RQ
A1	0.46	1.62	**A21**	0.56	2.86
A2	0.63	0.63	**A22**	0.45	1.72
A3	0.49	0.68	**A23**	0.59	1.29
A4	0.63	1.22	**A24**	0.65	1.33
A5	0.45	0.49	**A25**	0.87	1.12
A6	0.57	1.19	**B1**	0.41	1.01
A7	0.66	0.89	**B2**	0.62	0.90
A8	0.74	0.82	**B3**	0.37	0.76
A9	0.36	0.92	**B4**	0.41	0.52
A10	0.30	0.95	**B5**	0.57	0.48
A11	0.38	1.40	**B6**	0.34	0.62
A12	0.38	0.75	**B7**	0.40	0.80

A13	0.87	1.48	**B8**	0.38	0.74
A14	0.62	0.77	**B9**	0.42	0.86
A15	0.34	0.70	**B10**	0.34	0.59
A16	0.32	0.80	**B11**	0.26	0.97
A17	0.55	1.52	**B12**	0.26	1.01
A18	0.51	1.06	**B13**	0.27	0.67
A19	0.44	0.84	**B14**	0.31	0.99
A20	0.39	1.00			

Table 5. Relative quantity of TNFα and IL-1ß.

MNC-derived TNFα and IL-1ß expression

An analysis of variance showed that the effect of PCOS on TNFα and IL-1ß expression was significant, F(1,37) = 10.866, *P*=0.002 and F(1,37) = 7.588, *P*=0.009 respectively (**Figure 5**). A post hoc LSD test (**Figure 6**) showed a significant (*P*=0.003) difference between non-obese controls and obese PCOS, non-obese PCOS and obese controls were not significantly different from the other groups.

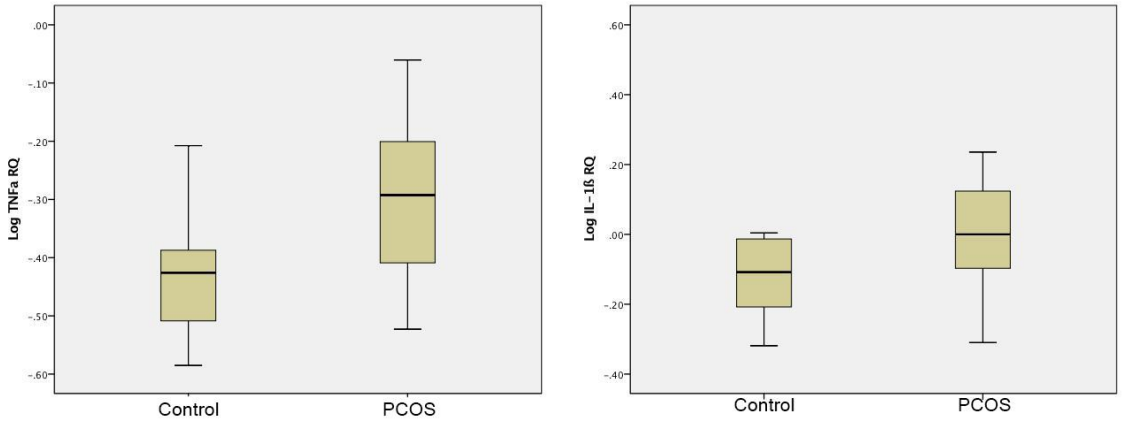

a **b**

Figure 5. Mononuclear Cell Cytokine Expression. Relative quantity of **a**, TNFα and **b**, IL-1ß from fasting samples. Significantly greater expression of TNFα (*P*=0.002) and IL-1ß (*P*=0.009) in women with PCOS compared to women without PCOS.

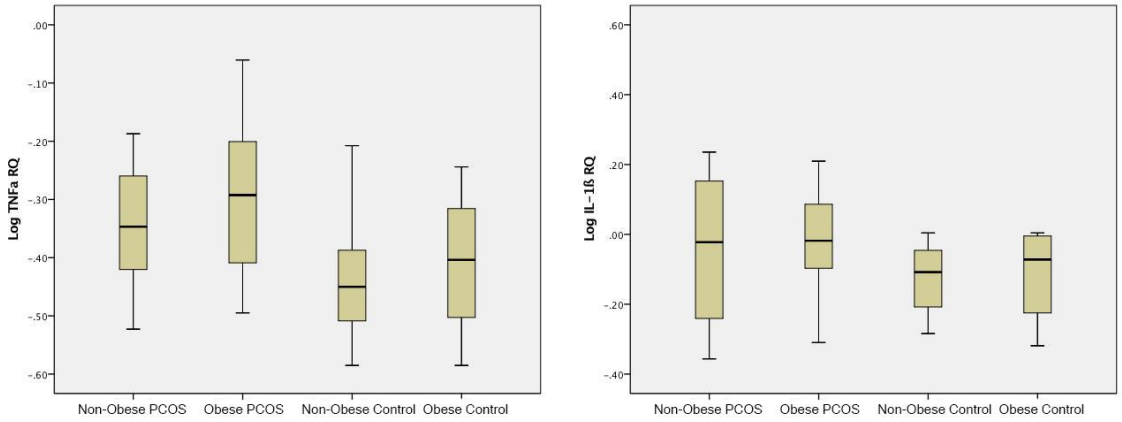

a **b**

Figure 6. Mononuclear Cell Cytokine Expression. Relative quantity of **a**, TNFα and **b**, IL-1ß from fasting samples. Expression of IL-1ß is significantly different between non-obese controls and obese PCOS (*P*=0.003).

A simple linear regression was calculated to predict TNFα and IL-1ß expression based on BMI for all study subjects. A significant regression equation was found (F(1,38) = 12.004, *P*=0.001), with an R^2=0.240 and (F(1,38) = 5.681, *P*=0.022), with an R^2=0.122 respectively.

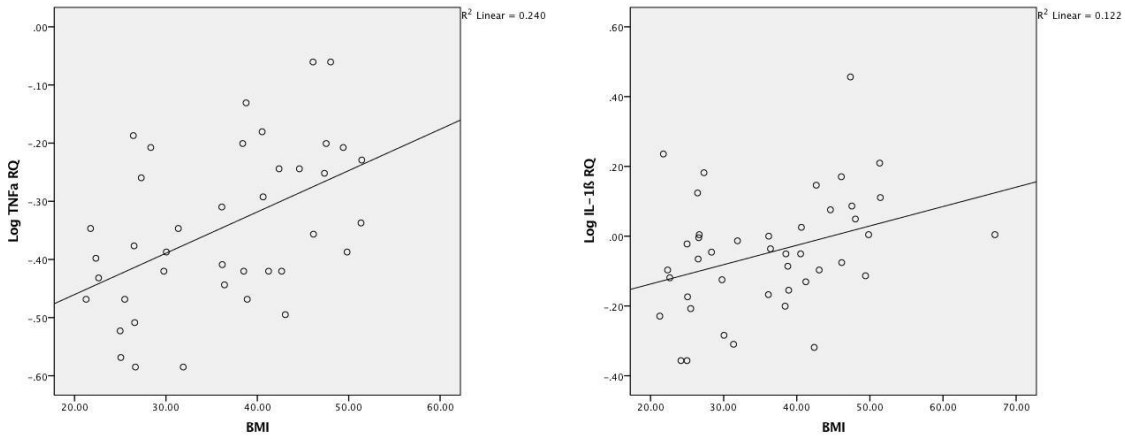

a **b**

Figure 7. Correlation Between BMI and Cytokine Expression. **a**, TNFα (*P*=0.001) **b**, IL-1ß (*P*=0.022).

A simple linear regression was calculated to predict TNFα and IL-1ß expression based on BMI among women with PCOS. An insignificant regression equation was found ($F(1,24) = 3.464$, $P=0.075$), with an $R^2=0.126$ for TNFα and ($F(1,24) = 2.881$, $P=0.101$), with an $R^2=0.096$ for IL-1ß.

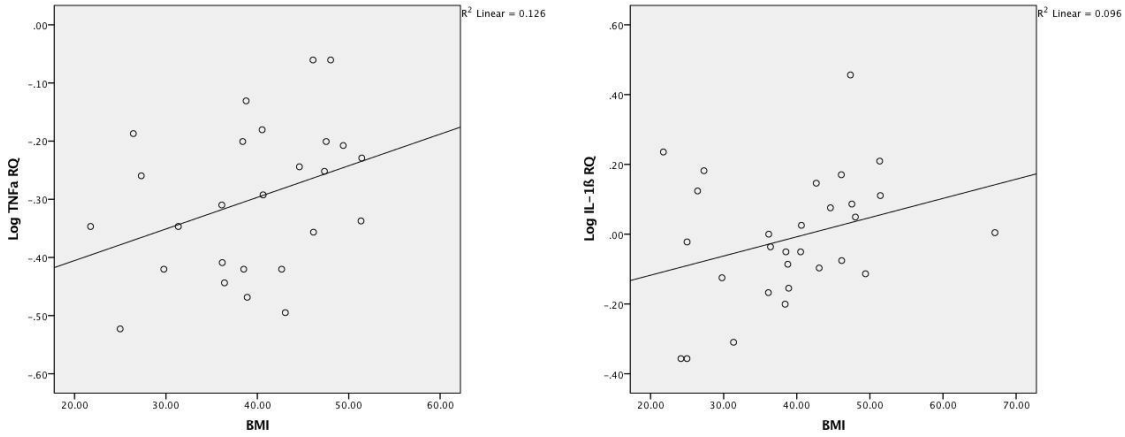

a **b**

Figure 8. Correlation between BMI of women with PCOS and cytokine expression. **a**, TNFα expression ($P=0.075$) and **b**, IL1ß expression ($P=0.101$).

A simple linear regression was calculated to predict TNFα and IL-1ß expression based on fasting glucose for all study subjects. A significant regression equation was found ($F(1,37) = 5.214$, $P=0.028$), with an $R^2=0.124$. An insignificant regression equation was found ($F(1,37) = 2.798$, $P=0.102$), with and $R^2=0.065$ for IL-1ß.

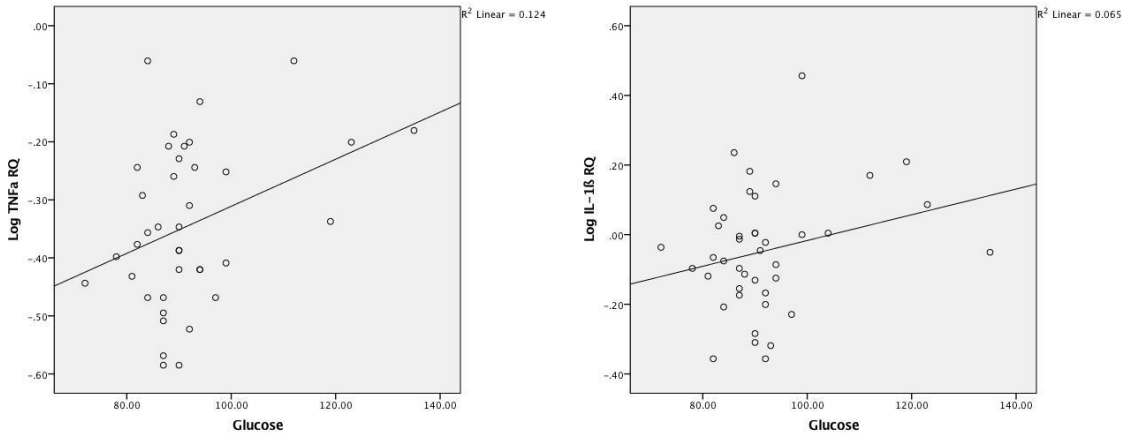

a **b**

Figure 9. Correlation between fasting glucose and cytokine expression. a, TNFα expression (*P*=0.028) and **b**, IL-1ß expression (*P*=0.102).

A simple linear regression was calculated to predict TNFα and IL-1ß expression based on fasting glucose for PCOS subjects. An insignificant regression equation was found (F(1,24) = 2.328, *P*=0.141, with an R^2=0.092 for TNFα and (F(1,24) = 1.625, *P*=0.214), with and R^2=0.059 for IL-1ß.

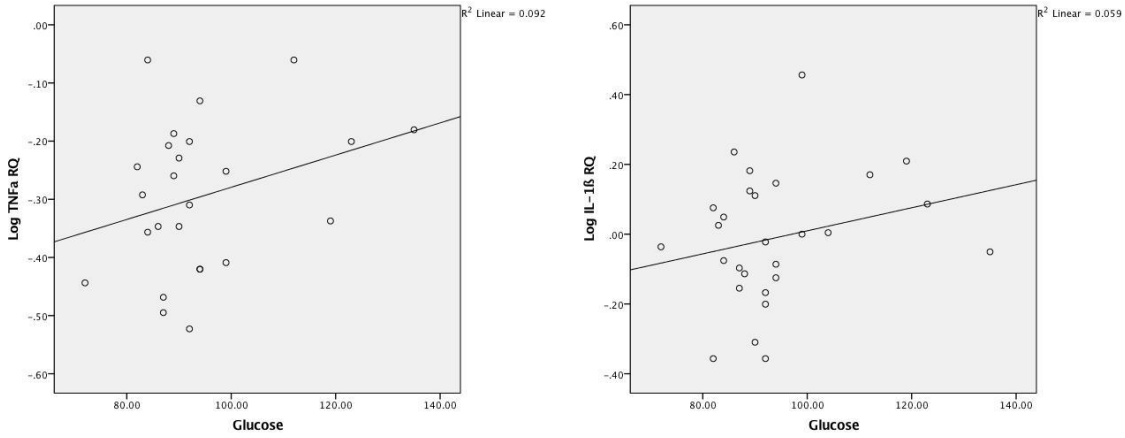

a **b**

Figure 10. Correlation between fasting glucose of women with PCOS and Cytokine Expression a, TNFα (*P*=0.141) **b**, IL-1ß (*P*=0.214).

Multiple linear regression analysis was calculated to predict TNFα and IL-1ß expression based on BMI and fasting glucose among women with PCOS. An insignificant regression was found ($F(2,22) = 2.329$, $P=0.121$) for TNFα, and $R^2=0.175$, and ($F(2,22) = 1.682$, $P=0.206$), and $R^2=0.119$ for IL-1ß. BMI and fasting glucose were not found to be significant predictors of TNFα and IL-1ß in women with PCOS.

CHAPTER IV

DISCUSSION

Polycystic ovarian syndrome is a common endocrine disorder in women of reproductive age and represents a complex pathophysiological model. Traditionally, PCOS has been characterized by the presence of excess androgens. However, excess androgens may be a secondary consequence of abnormal metabolic physiology. Obesity, a highly prevalent morbidity in women with PCOS, is well understood to contribute to an inflammatory environment leading to the development of insulin resistance. Although, a portion of women with PCOS remain who exhibit insulin resistance in the absence of obesity. Insulin resistance in the absence of obesity suggests an alternative mechanism mediating insulin sensitivity in women with PCOS. Recent evidence has suggested that that inflammatory dysregulation is a primary mediator leading to insulin resistance. Subsequent metabolic abnormalities resulting from impaired insulin sensitivity drives the clinical manifestation of excess androgens.

The effect of adiposity and fasting glucose on mRNA expression of TNFα and IL-1ß in MNCs was explored in women diagnosed with PCOS. Overexpression of both TNFα and IL-1ß are widely known to contribute to the development of glucose intolerance, insulin resistance, and atherosclerosis [18-20]. Data from this study gives evidence that mRNA expression of both TNFα and IL-1ß are increased in PCOS and

remains consistent with previous literature assaying protein. TNFα and IL-1ß mRNA was found to positively correlate with BMI in all study subjects, suggesting that BMI is a significant contributor of inflammation. However, a significant increase in TNFα and IL-1ß mRNA was not observed when only comparing PCOS subjects. Limitations in sample size may contribute to this observation. Although, BMI does not account for the distribution of adipose tissue in the individual. Preferential android adipose distribution may potentially contribute to the increased inflammatory environment observed in PCOS.

Correlations between fasting glucose and mRNA expression of TNFα and IL-1ß were also explored. Fasting glucose was observed to have little impact on TNFα and IL-ß mRNA expression in PCOS. However, a positive correlation was found between fasting glucose and TNFα among all study subjects. Plasma glucose concentration is heavily dependent on insulin concentration, and may inaccurately represent glycemic status by lowering plasma glucose if insulin is elevated. An improved model of glycemic status, homeostatic model assessment of insulin resistance (HOMA-IR), accounts for both glucose and insulin concentration.

Increased mRNA expression of TNFα and IL-1ß gives evidence that an inflammatory phenotype is predominant in PCOS. Inflammatory signals promote and maintain differentiation of macrophage towards the M1 phenotype. Maintaining an inflammatory environment significantly contributes to the development of insulin resistance and subsequent metabolic aberrations observed in PCOS.

Further research exploring inflammatory, and anti-inflammatory expression when challenged with a glucose load during a 3˚ glucose tolerance test may provide greater insight to the correlation between metabolic aberrations and inflammatory cytokine

expression. Inclusion of plasma insulin would provide a greater representation of glycemic status and insulin resistance of the subject. Also, measuring waist to hip circumference in addition to BMI may be a more significant indicator of adiposity than BMI alone.

In summary, this study provides evidence that mRNA expression of TNFα and IL-1ß is increased in women with PCOS. Therefore, inflammation is a significant pathophysiological component in PCOS that potentially plays a critical role in developing insulin resistance and hyperandrogenism.

REFERENCES

1. Roe, A.H. and A. Dokras, *The Diagnosis of Polycystic Ovary Syndrome in Adolescents.* Reviews in Obstetrics and Gynecology, 2011. **4**(2): p. 45-51.
2. Hart, R. and D.A. Doherty, *The potential implications of a PCOS diagnosis on a woman's long-term health using data linkage.* J Clin Endocrinol Metab, 2015. **100**(3): p. 911-9.
3. Hoffman, B.L., et al., *Polycystic Ovarian Syndrome and Hyperandrogenism*, in *Williams Gynecology, 3e*. 2016, McGraw-Hill Education: New York, NY.
4. Boyle, J. and H. Teede, *Polycystic ovary syndrome An update.* Australian Family Physician, 2012. **41**: p. 752-756.
5. Rojas, J., et al., *Polycystic ovary syndrome, insulin resistance, and obesity: navigating the pathophysiologic labyrinth.* Int J Reprod Med, 2014. **2014**: p. 719050.
6. Setji, T.L. and A.J. Brown, *Polycystic ovary syndrome: diagnosis and treatment.* Am J Med, 2007. **120**(2): p. 128-32.
7. Escobar-Morreale, H.F., et al., *Epidemiology, diagnosis and management of hirsutism: a consensus statement by the Androgen Excess and Polycystic Ovary Syndrome Society.* Hum Reprod Update, 2012. **18**(2): p. 146-70.
8. Pellatt, L., S. Rice, and H.D. Mason, *Anti-Mullerian hormone and polycystic ovary syndrome: a mountain too high?* Reproduction, 2010. **139**(5): p. 825-33.
9. Pierre, A., et al., *Loss of LH-induced down-regulation of anti-Mullerian hormone receptor expression may contribute to anovulation in women with polycystic ovary syndrome.* Hum Reprod, 2013. **28**(3): p. 762-9.
10. Blank, S.K., C.R. McCartney, and J.C. Marshall, *The origins and sequelae of abnormal neuroendocrine function in polycystic ovary syndrome.* Hum Reprod Update, 2006. **12**(4): p. 351-61.
11. Gonzalez, F., et al., *The altered mononuclear cell-derived cytokine response to glucose ingestion is not regulated by excess adiposity in polycystic ovary syndrome.* J Clin Endocrinol Metab, 2014. **99**(11): p. E2244-51.
12. Gonzalez, F., *Nutrient-Induced Inflammation in Polycystic Ovary Syndrome: Role in the Development of Metabolic Aberration and Ovarian Dysfunction.* Semin Reprod Med, 2015. **33**(4): p. 276-86.
13. Jensen, M.D., et al., *2013 AHA/ACC/TOS Guideline for the Management of Overweight and Obesity in Adults.* Circulation, 2014. **129**(25 suppl 2): p. S102-S138.
14. Flegal, K.M., et al., *Prevalence of obesity and trends in the distribution of body mass index among US adults, 1999-2010.* JAMA, 2012. **307**(5): p. 491-7.
15. Carmina, E., et al., *Abdominal fat quantity and distribution in women with polycystic ovary syndrome and extent of its relation to insulin resistance.* J Clin Endocrinol Metab, 2007. **92**(7): p. 2500-5.
16. Fauser, B.C., et al., *Consensus on women's health aspects of polycystic ovary syndrome (PCOS): the Amsterdam ESHRE/ASRM-Sponsored 3rd PCOS Consensus Workshop Group.* Fertil Steril, 2012. **97**(1): p. 28-38 e25.

17. Lord, J., et al., *The central issue? Visceral fat mass is a good marker of insulin resistance and metabolic disturbance in women with polycystic ovary syndrome.* BJOG, 2006. **113**(10): p. 1203-9.
18. Zhang, H., et al., *Role of TNF-alpha in vascular dysfunction.* Clin Sci (Lond), 2009. **116**(3): p. 219-30.
19. Willerson, J.T. and P.M. Ridker, *Inflammation as a cardiovascular risk factor.* Circulation, 2004. **109**(21 Suppl 1): p. II2-10.
20. Maedler, K., et al., *Interleukin-1 beta targeted therapy for type 2 diabetes.* Expert Opinion on Biological Therapy, 2009. **9**(9): p. 1177-1188.
21. Moganti, K., et al., *Hyperglycemia induces mixed M1/M2 cytokine profile in primary human monocyte-derived macrophages.* Immunobiology, 2016.
22. Crowther, M., et al., *Microenvironmental influence on macrophage regulation of angiogenesis in wounds and malignant tumors.* Journal of Leukocyte Biology, 2001. **70**(4): p. 478-490.
23. Kittan, N.A., et al., *Cytokine induced phenotypic and epigenetic signatures are key to establishing specific macrophage phenotypes.* PLoS One, 2013. **8**(10): p. e78045.
24. Rice, K.L., I. Hormaeche, and J.D. Licht, *Epigenetic regulation of normal and malignant hematopoiesis.* Oncogene, 2007. **26**(47): p. 6697-714.
25. McNelis, J.C. and J.M. Olefsky, *Macrophages, immunity, and metabolic disease.* Immunity, 2014. **41**(1): p. 36-48.
26. Olefsky, J.M. and C.K. Glass, *Macrophages, inflammation, and insulin resistance.* Annu Rev Physiol, 2010. **72**: p. 219-46.
27. Odegaard, J.I., et al., *Alternative M2 activation of Kupffer cells by PPARdelta ameliorates obesity-induced insulin resistance.* Cell Metab, 2008. **7**(6): p. 496-507.
28. Goh, Y.P.S., et al., *Eosinophils secrete IL-4 to facilitate liver regeneration.* Proceedings of the National Academy of Sciences of the United States of America, 2013. **110**(24): p. 9914-9919.
29. Wu, D., et al., *Eosinophils sustain adipose alternatively activated macrophages associated with glucose homeostasis.* Science, 2011. **332**(6026): p. 243-7.
30. Biswas, S.K. and A. Mantovani, *Orchestration of metabolism by macrophages.* Cell Metab, 2012. **15**(4): p. 432-7.
31. Daneman, D., et al., *Insulin-Stimulated Glucose Transport in Circulating Mononuclear Cells From Nondiabetic and IDDM Subjects.* Diabetes, 1992. **41**(2): p. 227.
32. Flier, J.S., et al., *Impaired in Vivo Insulin Clearance in Patients With Severe Target-Cell Resistance to Insulin.* Diabetes, 1982. **31**(2): p. 132.
33. Gao, Z., et al., *Serine phosphorylation of insulin receptor substrate 1 by inhibitor kappa B kinase complex.* J Biol Chem, 2002. **277**(50): p. 48115-21.
34. Zhang, J., et al., *S6K directly phosphorylates IRS-1 on Ser-270 to promote insulin resistance in response to TNF-(alpha) signaling through IKK2.* J Biol Chem, 2008. **283**(51): p. 35375-82.
35. Donath, M.Y. and S.E. Shoelson, *Type 2 diabetes as an inflammatory disease.* Nat Rev Immunol, 2011. **11**(2): p. 98-107.

36. Welty, F.K., A. Alfaddagh, and T.K. Elajami, *Targeting inflammation in metabolic syndrome.* Transl Res, 2016. **167**(1): p. 257-80.
37. Mohanty, P., et al., *Glucose Challenge Stimulates Reactive Oxygen Species (ROS) Generation by Leucocytes.* The Journal of Clinical Endocrinology & Metabolism, 2000. **85**(8): p. 2970-2973.
38. Baptiste, C.G., et al., *Insulin and hyperandrogenism in women with polycystic ovary syndrome.* J Steroid Biochem Mol Biol, 2010. **122**(1-3): p. 42-52.
39. Lauretta, R., et al., *Insulin-Sensitizers, Polycystic Ovary Syndrome and Gynaecological Cancer Risk.* Int J Endocrinol, 2016. **2016**: p. 8671762.
40. Wu, S., et al., *Obesity-Induced Infertility and Hyperandrogenism Are Corrected by Deletion of the Insulin Receptor in the Ovarian Theca Cell.* Diabetes, 2014. **63**(4): p. 1270.
41. Jamnongjit, M. and S.R. Hammes, *Ovarian Steroids: The Good, the Bad, and the Signals that Raise Them.* Cell cycle (Georgetown, Tex.), 2006. **5**(11): p. 1178-1183.
42. Gonzalez, F., et al., *Elevated serum levels of tumor necrosis factor alpha in normal-weight women with polycystic ovary syndrome.* Metabolism, 1999. **48**(4): p. 437-441.
43. Dumesic, D.A., et al., *Hyperandrogenism Accompanies Increased Intra-Abdominal Fat Storage In Normal Weight Polycystic Ovary Syndrome Women.* J Clin Endocrinol Metab, 2016: p. jc20162586.
44. Gonzalez, F., et al., *Evidence of mononuclear cell preactivation in the fasting state in polycystic ovary syndrome.* Am J Obstet Gynecol, 2014. **211**(6): p. 635 e1-7.
45. Jensterle Sever, M., et al., *Short-term combined treatment with liraglutide and metformin leads to significant weight loss in obese women with polycystic ovary syndrome and previous poor response to metformin.* Eur J Endocrinol, 2014. **170**(3): p. 451-9.
46. Pfaffl, M.W., *A new mathematical model for relative quantification in real-time RT–PCR.* Nucleic Acids Research, 2001. **29**(9): p. e45-e45.

APPENDIX

Sample	Age (y)	BMI (kg/m^2)	Glucose (mg/dL)
A1	30	51.3	119
A2	32	38.4	92
A3	39	36.1	92
A4	37	47.5	123
A5	33	31.3	90
A6	26	44.6	82
A7	33	40.5	135
A8	37	38.8	94
A9	29	36.4	72
A10	19	25.0	92
A11	47	42.7	94
A12	40	29.8	94
A13	26	46.1	112
A14	28	49.4	88
A15	21	38.9	87
A16	35	43.1	87
A17	48	27.3	89
A18	24	40.6	83
A19	22	46.1	84
A20	22	36.2	99
A21	33	47.3	99
A22	36	21.8	86
A23	42	51.4	90
A24	55	26.4	89
A25	21	48.0	84
B1	39	49.8	90
B2	25	28.3	91
B3	18	22.6	81
B4	20	30.0	90
B5	23	42.4	93
B6	18	25.5	84
B7	18	22.3	78
B8	18	41.2	90
B9	18	26.5	82
B10	18	21.3	97
B11	18	31.9	87
B12	18	26.7	90

B13	20	25.1	87
B14	18	26.6	87

Appendix 1. Age, BMI, and fasting glucose